

Molecular dynamics study of lattice kink diffusion

J. Andrew Combs and Sidney Yip

Department of Nuclear Engineering, Massachusetts Institute of Technology, Cambridge, Massachusetts 02139

(Received 25 April 1983)

Single-kink diffusion is simulated in a ϕ^4 lattice by the method of molecular dynamics. The temperature dependence of the single-kink diffusion constant D_K is obtained from the kink mean-square displacement and velocity autocorrelation function. When system parameters are chosen such that discrete lattice effects are significant, kink diffusion is found to be a random-walk process that requires thermal activation of the kink over its Peierls barrier. Short-time behavior of the kink velocity autocorrelation function reveals trapped oscillations and damped propagation of the kink.

I. INTRODUCTION

A great deal of theoretical effort has been expended in the last ten years in order to understand the nature of the density correlation spectrum $S(q, \omega)$ observed in neutron inelastic scattering from ferroelectrics near their structural phase transitions. $S(q, \omega)$ exhibits an anomalously intense and narrow central peak in addition to soft modes and the normal phonon spectrum. It has been hypothesized¹⁻⁵ that the central peak phenomenon is due to the motion of localized density fluctuations commonly referred to as kinks or domain walls.

One of the simplest model systems that supports kinks is a one-dimensional bistable lattice traditionally known as the ϕ^4 lattice. It is the model most commonly studied in connection with ferroelectrics. Its Hamiltonian is given by

$$H = \sum_l m \frac{\dot{u}_l^2}{2} + \sum_l \frac{C}{2} (u_{l+1} - u_l)^2 + \sum_l V_R(u_l), \quad (1.1)$$

where u_l is the displacement of the l th particle away from its mean position $x_l = lb$, C is a Hooke's law interatomic coupling constant, and V_R is the single-particle ϕ^4 potential

$$V_R(u) = -\frac{A}{2}u^2 + \frac{B}{4}u^4. \quad (1.2)$$

V_R has two minima at $u_0 = \pm\sqrt{|A|/B}$, separated by an energy barrier $E_0 = A^2/4B$. Note that (1.1) is simply a linear chain of atoms with near-neighbor coupling subject to the double-well potential V_R .

The quartic term in V_R gives rise to a cubic nonlinearity in the equations of motion which makes analysis extremely difficult. The method of molecular dynamics has been used, therefore, to obtain solutions of (1.1). At temperatures $T \lesssim E_0/k_B$, where k_B is Boltzmann's constant, atoms execute small-amplitude thermal motions about the minima of V_R . Neighboring atoms tend to align, but the desire of the system to maximize entropy causes atoms to occupy opposite wells. This results in large amplitude kinks in the atomic displacement profile which connect neighboring domains of atoms aligned in opposite wells. Calculations of $S(q, \omega)$ from these solutions reveal an intense quasielastic central peak which is not present in the absence of these kinks.¹ These calculations encouraged development of a theoretical understanding of (1.1), its

kink solutions, and the nature of their interactions with fluctuations.

Progress has been made in the development of a well-defined kink mechanics. Typically the continuum approximation is invoked to reduce the N -body Hamiltonian (1.1) to a wave equation called the ϕ^4 field equation. Kinks exist as particular solutions of the ϕ^4 field equation which are stable to small fluctuations. The continuum theory has been used to show that both free² and diffusive^{4,5} kink motions lead to a central peak in $S(q, \omega)$.

The continuum theory, however, suffers from an inherent weakness. The continuum approximation is valid only for $\tilde{C} \gg 1$, where

$$\tilde{C} \equiv \frac{C}{A} \quad (1.3)$$

is the nondimensional interatomic coupling parameter. There is evidence^{5,6} that kinks in some ferroelectric materials are not appropriately described by the continuum theory; i.e., $\tilde{C} < 1$. It has been shown that for $\tilde{C} < 1$ significant effects of lattice discreteness appear in the kink motion, and that many interesting and important kink phenomena are manifest only when the fully discrete problem is analyzed.⁶⁻⁸ Strong kink-fluctuation coupling due to discreteness gives rise to such phenomena as strong kink damping and lattice trapping of kinks.⁶⁻⁸ These effects increase as \tilde{C} is decreased. They essentially dominate kink motion for $\tilde{C} < 1$. Thus, it is not clear that the results of continuum theory are entirely appropriate in a discussion of ferroelectric phase transformations.

Since exact solutions of the lattice theory are not available,⁶ and since the continuum theory itself is not applicable in many cases of interest, we follow a numerical approach in which atomic trajectories of the ϕ^4 lattice are generated by molecular dynamics simulation. In this way the full effects of discreteness upon kink motion are retained. The model system contains only a single kink. This condition is maintained by imposing an antiperiodic boundary condition on a finite-size chain, and restricting the simulation to sufficiently low temperatures that kink nucleation does not occur. The kink coordinate is extracted by analyzing the system configuration in terms of a kink structure plus fluctuations.^{6,7} Statistical properties of the kink are then examined through time-correlation functions constructed from the kink coordinates.

Calculations of the kink velocity autocorrelation function, its spectrum, and the kink mean-square displacement function reveal that kink motion is diffusive at $\tilde{C} < 1$. Discrete lattice effects dominate kink motions in this regime. The kink exhibits behavior dominated by trapped oscillations at low T , and dissipative propagation at high T . Lattice "friction" is always significant in the low \tilde{C} regime, so that the kink never approaches free motion, even as $T \rightarrow 0$. The statistical dynamics of kinks at $\tilde{C} < 0.5$ can be characterized as activated Brownian motion. The resulting diffusion constant is approximately linear in temperature (the typical Brownian particle result) weighted by an Arrhenius factor.

The value of the kink diffusion constant calculated from our model at \tilde{C} values characteristic of lead germanate and antimony sulfide is extremely small. This yields extremely small values for the width of a diffusive central peak in $S(q, \omega)$, smaller than obtainable by present neutron spectrometer resolution. It is asserted, therefore, that intrinsic effects of lattice discreteness are sufficient to account for the anomalously narrow and intense character of the central peak phenomenon observed in $S(q, \omega)$ near ferroelectric phase transformations.

II. SIMULATION OF THERMAL KINK MOTION

The equations of motion to be studied are obtained from (1.1), and in dimensionless forms are

$$\frac{\partial^2 \tilde{u}_l(\tilde{t})}{\partial \tilde{t}^2} - \tilde{c} [\tilde{u}_{l+1}(\tilde{t}) + \tilde{u}_{l-1}(\tilde{t}) - 2\tilde{u}_l(\tilde{t})] - \tilde{u}_l(\tilde{t}) + \tilde{u}_l^3(\tilde{t}) = 0, \quad (2.1)$$

where

$$\begin{aligned} u_l &= u_0 \tilde{u}_l, \\ t &= \tau \tilde{t}, \\ \tau &= \sqrt{m/A}. \end{aligned}$$

We also define the following nondimensional quantities:

$$\begin{aligned} X &= b\tilde{X}, \quad T = \frac{A^2}{k_B B} \tilde{T}, \\ K &= \frac{1}{b} \tilde{K}, \quad M = m \frac{u_0^2}{b^2} \tilde{M}, \\ \Gamma &= \frac{1}{\tau} \tilde{\Gamma}, \quad D_K = \frac{b^2}{\tau} \tilde{D}_K, \\ E_a &= \frac{A^2}{B} \tilde{E}_a, \quad c_0 = \frac{b}{\tau} \tilde{c}_0. \end{aligned}$$

$X(t)$ is the time-dependent kink position, K is its inverse width (or wave number), Γ is the phenomenological friction constant, E_a is the energy barrier to kink motion (the Peierls barrier), M is the kink mass, D_K is the single-kink diffusion coefficient, and c_0 is the sound speed. The origins of Γ and E_a have been studied previously by the authors.⁷ Note that E_a is different from the kink formation energy $E_0 = Mc_0^2$. All frequencies will be nondimensionalized by $1/\tau$. Henceforth, the tildes will be suppressed except in the case of \tilde{C} where it will be retained to avoid

confusion.

Applying the standard molecular dynamics techniques,⁹ the equations of motion are integrated numerically using a central difference scheme. A time step size of $\Delta t = 0.05$ is chosen. This is sufficient to ensure that the atomic trajectories are reproducible to within 0.1% over an interval of $t = 500$. This interval is more than 10 times longer than a typical time required for equilibration.

The simulation begins with the particles arranged such that a single kink exists in the system. To ensure that additional kinks are not created T is kept to low values. It is found that for $T \leq 0.1$, for the system size chosen (see below), kink formation does not occur.⁷ Because the conventional periodic boundary condition would always produce an even number of kinks, an "antiperiodic" boundary condition is imposed,

$$u_0 \equiv -u_N, \quad u_{N+1} \equiv -u_1. \quad (2.2)$$

The kink position $X(t)$ is determined from the atomic displacements by first separating the total amplitude u_l into a single kink plus fluctuations,

$$u_l(t) = u_k^l(X(t)) + \phi_l(t), \quad (2.3)$$

where $u_k^l(X) = \tanh[K(x_l - X)]$ and $K = 1/(2\tilde{C})^{1/2}$ characterizes the kink wave form, and $\phi_l(t)$ are the fluctuations. The quantity X is allowed to become a dynamic variable. Given $u_l(t)$ for $l = 1, \dots, N$, we have N equations (2.1) in $N + 1$ unknowns $\phi_l(t)$ and $X(t)$. To determine the solution uniquely we invoke the additional constraint,¹⁰

$$\sum_l \frac{\partial u_k^l}{\partial X} \phi_l = 0, \quad (2.4)$$

which has the effect of minimizing $\phi_l(t)$ in the domain-wall region (where du_k/dx peaks). Thus, given the positions $u_l(t)$ from numerical integration, X can be varied using (2.3) until (2.4) is satisfied within an acceptable error by finding the root of (2.4) numerically. The $X(t)$ is obtained and stored for use later in calculating the mean-square displacement and the velocity autocorrelation function.

To minimize statistical fluctuations time-correlation-function results are averaged over a number of time origins, typically 500. For a given \tilde{C} and T , up to 100 different trajectories were generated, each corresponding to a different microstate of the system. The different trajectories then allow an estimate of the statistical uncertainty in the various dynamical quantities computed.

All the simulation results presented here are obtained with $N = 200$.⁶ This chain length is considered reasonable from the standpoint of computational cost and of minimizing the distortion from a fully relaxed kink configuration. For $N = 200$ the time it takes a fluctuation to traverse the system is $200/c_0$. It turns out that $c_0 = (\tilde{C})^{1/2}$. With $\tilde{C} = 0.5$, $c_0 = 0.707$, so that the traversal time is 270; this time is generally greater than the time interval of $t \sim 200$ over which we will be examining most of the time correlation functions.

In choosing the values of C and T for simulation we are guided by the fact that the larger the \tilde{C} value the less

resistance there is for the kink to move through the lattice. It has been found that with $\tilde{C} \lesssim 1$ a moving kink will slow down and become trapped by the lattice within a reasonable computational time. Since our interest is in the diffusive motion of a localized kink, we have chosen to work mostly with $\tilde{C}=0.5$; however, additional runs are also made at $\tilde{C}=0.2$ and $\tilde{C}=0.7$.

The choice of T is partly dictated by the condition of no kink creation. But also the system behaves differently depending on whether or not $T > E_a$. For $\tilde{C}=0.5$, the zero-temperature value of E_a is 0.022.⁷ The range of T investigated is, therefore, chosen to be about this energy value, from $T=0.005$ to 0.087.

III. TIME CORRELATION FUNCTIONS AND KINK DIFFUSION

The mean-square displacement function,

$$W(t) = \langle [(X(t) - X(0))]^2 \rangle, \quad (3.1)$$

is a fundamental quantity in the discussion of self-diffusion. Its slope at long times gives the self-diffusion coefficient,

$$D_k = \lim_{t \rightarrow \infty} \frac{W(t)}{2t}. \quad (3.2)$$

$W(t)$ is directly related to the velocity autocorrelation function $\langle V(t)V(0) \rangle$ whose time integral is the diffusion constant,

$$D_k = \int_0^\infty dt \langle V(t)V(0) \rangle. \quad (3.3)$$

One may also determine the diffusion constant from the Fourier transform

$$\hat{\psi}(\omega) = 2 \int_0^\infty dt \cos \omega t \langle V(t)V(0) \rangle. \quad (3.4)$$

Then the diffusion constant is just

$$D_k = \frac{\hat{\psi}(0)}{2}. \quad (3.5)$$

The simulation results for $W(t)/2t$ are plotted in Fig. 1, and the long-time limit (3.2) is obtained graphically. It can be seen that asymptotic behavior has not been reached in the case of $T=0.005$, but for all higher temperatures the ratio $W(t)/2t$ has reached a constant in the time of observation.

The single-kink diffusion constants obtained in Fig. 1 are plotted as a function of temperature in Fig. 2. Errors are estimated from the difference of results obtained from (3.3) and (3.5) (see Fig. 4) increased by the errors in graphical determination. The solid curve is calculated from the function

$$D_k = (T/M\Gamma) \exp(-E_a/T). \quad (3.6)$$

The zero-temperature \tilde{C} dependence of these parameters are determined to be⁷

$$M = \frac{2\sqrt{2}}{3\sqrt{\tilde{C}}}, \quad (3.7a)$$

$$\Gamma = 5.28 \exp(-7.5\tilde{C}), \quad (3.7b)$$

$$E_a = 0.25 \exp(-4.84\tilde{C}). \quad (3.7c)$$

These will be called the "zero-temperature" values of the kink mass, lattice friction constant, and Peierls barrier, respectively. At $\tilde{C}=0.5$ we find that $M=1.33$, $\Gamma=0.124$, and $E_a=0.022$. When these values are inserted into (3.6) the solid curve in Fig. 2 results. One might recall that the diffusion constant for the Brownian motion of a particle of mass M is just $\langle V^2 \rangle / \Gamma$. The form of (3.6) includes an additional activation factor.

The explicit \tilde{C} and T dependence of D obtained from the insertion of (3.7) in (3.6) is

$$D_k = 0.2009 \sqrt{\tilde{C}} T \exp \left[-7.5\tilde{C} - \frac{e^{-4.84\tilde{C}}}{T} \right]. \quad (3.8)$$

When the value of D_k is obtained for $\tilde{C}=0.2$ and $T=0.02$ the prediction of (3.8) is 0.00007 and the observed value is 0.00014 ± 0.00007 , which is within the statistical error; but for $\tilde{C}=0.7$ and $T=0.097$, (3.8) yields 2.84, and the observed value is 1.5 ± 0.7 , which is outside the range of error. The latter discrepancy could be due purely to poor statistics. It is expected, however, that as \tilde{C} increases memory effects in the kink motion will become significant.⁴ Thus, the simple model of memoryless dissipation which yields the diffusion law (3.6) would become less and less applicable as the continuum (high- \tilde{C}) limit is approached. This would result in deviations from (3.6) as \tilde{C} is increased. Since (3.6) is good for $\tilde{C} < 0.5$, and the discrepancy occurs at $\tilde{C}=0.7$, we believe that we are seeing effects of the transition from low- \tilde{C} to high- \tilde{C} behavior.

The normalized velocity autocorrelation function $\psi(t)$ may be defined as

$$\psi(t) = \frac{\langle V(t)V(0) \rangle}{\langle V^2 \rangle}. \quad (3.9)$$

Since this quantity is well defined whether or not the kink is undergoing diffusive motion, an examination of the short-time behavior of $\psi(t)$ can reveal a good deal about the local kink dynamics.

The only continuum theory that yields predictions of (3.9) [and (3.4)] is that of Sahni and Mazenko.⁴ Their kink velocity autocorrelation exhibits significant memory effects, a long time tail, and an oscillation due to kink-phonon coupling. This yields a $\hat{\psi}(\omega)$ with central and side peaks. The side peak occurs at a frequency of $\sqrt{2}$ regardless of the T or \tilde{C} of the system. The central peak is diffusive in nature, although distinctly different from a simple Lorentzian which characterizes Brownian motion. It is of interest to compare their continuum prediction to the observed behavior of kinks in the low \tilde{C} regime.

The simulation data for (3.9) are shown in Fig. 3 at various temperatures. It is apparent that there are two distinct regions of characteristic behavior: a low-temperature region ($T < E_a$) where distinct oscillations in $\psi(t)$ correspond to vibrational motions in a trapped configuration, and a high-temperature region ($T > E_a$) where smooth monotonic decay of $\psi(t)$ indicates a continuous kink motion away from its initial position.

This behavior is even more striking when $\hat{\psi}(\omega)$ is plotted (Fig. 4). The points result from a Fourier transform

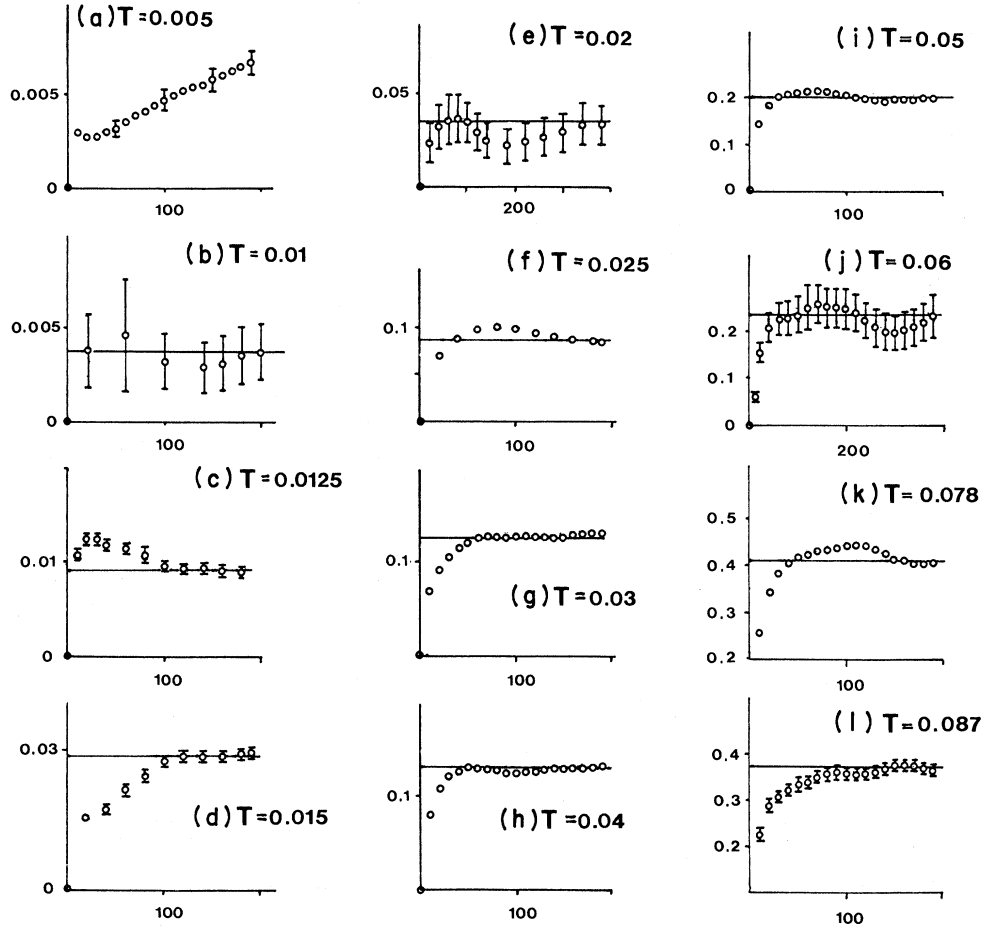


FIG. 1. $W(t)/2t$ for $\tilde{C}=0.5$ at various temperatures. Solid lines represent the graphical estimate of the long-time limit. Error bars denote the standard error.

of the raw data. This reveals the diffusive (central peak) and oscillatory (side peak) aspects of the motion.

The position ω_0 of the oscillatory peak depends upon C (Ref. 7)

$$\omega_0^2 = \frac{2\pi^2 E_a}{M}. \quad (3.10)$$

For $\tilde{C}=0.5$, ω_0 is 0.57. There is a peak splitting, presumably due to nonlinear kink-phonon coupling. The oscillatory peak rapidly disappears above $T=E_a$. A comparison of $\hat{\psi}(\omega)$ for different \tilde{C} values in Fig. 5 shows that the oscillatory peak position is well predicted by (3.10). Thus, the presence of trapped oscillations of the kink due to discrete lattice effects is confirmed. The oscillatory peak predicted by Sahni and Mazenko is of a wholly different character than the one just discussed. Some evidence for "continuum" peak does exist in these simulations. In Fig. 5(a), the $\hat{\psi}(\omega)$ for $\tilde{C}=0.7$ is carried out to $\omega=1.5$, and reveals a small bump in the data. Although one might normally consider this noise, the same bump (about 5% above the background) occurred at $\omega=\sqrt{2}$ in nearly all simulations for $T>E_a$, and disappeared for $T<E_a$. This is precisely the behavior one would expect for this phenomena, which only occurs when the kink is in the propagating regime (treated by the continuum theory). In any case, the oscillatory peak of the continuum theory is a rather minor

effect at these low \tilde{C} values.

The diffusion constant can be obtained from the height $\hat{\psi}(0)$ of the central peak [cf. (3.5)], and one can see that these values compare well with those plotted in Fig. 1. The value of Γ is just the width of the central peak. These results clearly point to the concept that kink diffusion is an activated process, requiring a fluctuation energy comparable to the barrier height E_a .

The curves in Figs. 3–5 are calculated from a two-parameter fit to a simple two-state model which contains the features of trapped oscillation and dissipative propagation.^{8,11} The velocity autocorrelation function in this model is determined from limiting behavior in the propagating "H" (high-velocity) and oscillatory "L" (low-velocity) regimes

$$\psi(t) \cong \psi_H(t)P_H + \psi_L(t)(1-P_H). \quad (3.11)$$

P_H is probability for occupation of the propagation regime, and we set

$$P_H = e^{-E_a/T}. \quad (3.12)$$

We will allow E_a to vary from its zero-temperature value (3.7c). The H regime is just a Brownian diffusion regime, and the L regime is just a dissipative oscillatory regime; thus, we may write¹¹

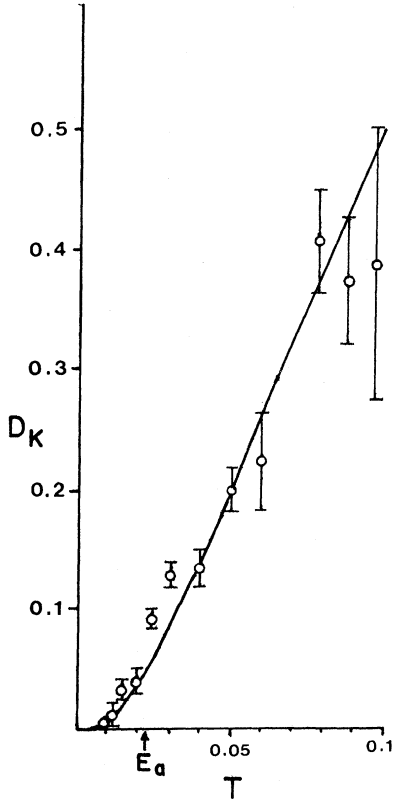


FIG. 2. Single kink diffusion constant D_K for $\tilde{C}=0.5$ at various temperatures. Circles are molecular-dynamics data. Curve is Eq. (3.6) evaluated at the zero-temperature values (3.7).

$$\psi_H(t) = e^{-\Gamma t}, \quad (3.13)$$

$$\psi_L(t) = e^{-\Gamma t/2} \left[\cos(\omega_1 t) - \frac{\Gamma}{2\omega_1} \sin(\omega_1 t) \right], \quad (3.14)$$

where

$$\omega_1^2 = \omega_0^2 + \frac{\Gamma^2}{4}. \quad (3.15)$$

The value of Γ will also be allowed to vary from its zero-temperature value (3.7b). The diffusion constant D_k deduced from this model is just

$$D_k = \frac{\langle V^2 \rangle}{\Gamma} e^{-E_a/T} \quad (3.16)$$

which is identical to (3.6) when $\langle V^2 \rangle = T/M$. The $\hat{\psi}(\omega)$ that results from the Fourier transform of (3.13) and (3.14) are Lorentzian peaks, centered about zero and ω_1 , respectively.

The high-temperature regime ($T > E_a$) reveals nearly exponential decay of $\psi(t)$ in Fig. 3 and Lorentzian behavior of the central peak of $\hat{\psi}(\omega)$ in Fig. 4. This suggests that the diffusive peak in this regime is basically due to memoryless dissipative mechanisms of a simple Brownian type. The high- T regime is also characterized by Γ 's and E_a 's which deviate from their zero-temperature

values; however, the D_k values calculated from the temperature-dependent values do not significantly differ from those plotted in Fig. 2.⁶

The low- T regime apparently has a great deal more structure than predicted in our simple model. There exist very-low-frequency peaks significantly above the background, which appear real. This also may suggest memory effects in kink dissipation.

IV. KINK DIFFUSION IN OTHER MODELS AND TWO FERROELECTRIC MATERIALS

There have been a number of previous attempts to predict the single-kink diffusion constant of the ϕ^4 lattice, all of which use the continuum approximation. The predictions of Sahni and Mazenko,⁴ Wada and Schreiffer,³ and Collins *et al.*⁵ are presented as follows:

$$D_k = \frac{\sqrt{2}}{3} k^{7/2} T^{1/2} \tilde{C}^{5/4}, \quad (4.1)$$

$$D_k = \frac{0.516\sqrt{2}}{4} T^2, \quad (4.2)$$

$$D_k = \frac{\langle V^2 \rangle}{\lambda} = \frac{T}{\lambda M}. \quad (4.3)$$

If λ is set equal to Γ then (3.16) and (4.3) coincide in the continuum limit since E_a goes rapidly to zero [cf. (3.7c)]. If we were to plot (4.1) and (4.2) on Fig. 2, the curves would be indistinguishable from the vertical and horizontal axes, respectively. Strictly speaking, λ is zero in the ϕ^4 lattice (it is extrinsic rather than intrinsic in origin), so that (4.3) diverges. Thus, the continuum-theory results for diffusion certainly do not apply for $\tilde{C} < 0.5$, and probably not for $\tilde{C} < 1$.

If it can be assumed that the numbers obtained for one-dimensional kink models are applicable to real ferroelectric systems, then it turns out that low C values are important when comparison with experimental results is made. In the work of Currie *et al.*⁵ results of experimental studies of ferroelectrics lead germanate and antimony sulphide, which exhibit structural phase transitions and the central peak effect, were compiled and related to ϕ^4 lattice parameters. Using their compilations for the values of molecular mass m , sound speed c_0 , lattice constant b , and force constant A , and noting that $mc_0^2 = Cb^2$, where C is now taken to be dimensional as in (1.1), \tilde{C} for the two ferroelectrics are 0.336 and 0.081, respectively. These are extremely low \tilde{C} values where discreteness effects such as kink localization and thermally activated diffusion are expected to dominate. The temperatures of structural phase transition are 0.0023 and 0.0030, respectively, both of which are in the localization regime. Domain walls of higher dimension tend to be even more localized, since lines or surfaces define domain walls and the random tensions generated by thermal motions on the wall will tend to cancel, thereby restricting net domain-wall motion. Thus, we assert that the intrinsic mechanisms which tend to localize domain walls in a lattice should be quite sufficient to produce the extremely narrow central peaks observed near ferroelectric phase transformations.

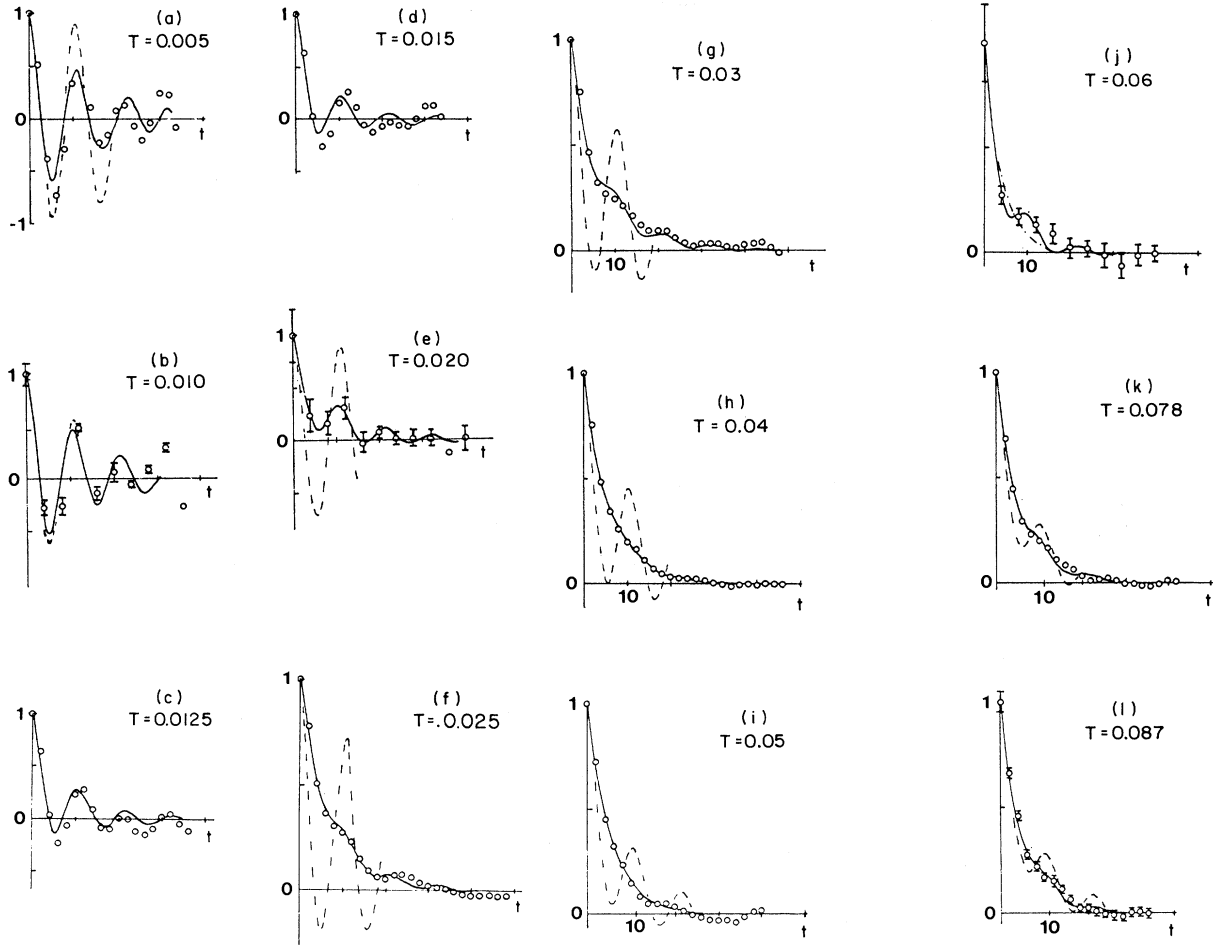


FIG. 3. Normalized kink velocity autocorrelation function $\psi(t)$ for $\tilde{C}=0.5$ at various temperatures. Circles are molecular dynamics data. Solid curves are from Eqs. (3.11)–(3.14) where both E_a and Γ are fit to the data; dashed curves utilize the zero-temperature value of E_a and fit only Γ , except for (j) where the dashed curve is a simple exponential fit. Division marks on time axis denote intervals of 10τ .

V. CONCLUSION

Results of molecular dynamics calculations show that activated diffusion of single kinks in a one-dimensional ϕ^4 lattice takes place at $\tilde{C} < 0.7$. The single-kink diffusion constant is well represented by a Brownian diffusion prefactor (linear in temperature T) weighted by an Arrhenius probability factor. The latter arises due to discrete lattice effects which causes the kink energy to vary periodically with the lattice spacing; thus to propagate through the lattice, a kink localized between lattice sites must be activated over its barrier E_a . Although the diffusion constant is difficult to obtain for higher \tilde{C} values, such molecular dynamics calculations would be of substantial value to test the limits of applicability of the expression (3.6), and the nature of diffusion as the transition to continuum behavior is made.

A number of questions remain to be resolved in future thermal lattice kink studies. The nature of the temperature dependence of the phenomenological friction Γ , kink mass, and energy barrier height E_a remains unclear. Some deviations from their zero-temperature values apparently exist when one examines the diffusion-constant data, and these deviations need clarification. The \tilde{C} dependence of the temperature-dependent part of E_a is of particular importance. A detailed study of the mean kink profile in the thermal lattice is of interest. The mean kink profile should give insight into the effective kink mass, which depends upon the kink width and shape. The exact nature of the systematic and random forces that affect the kink due to fluctuations should be investigated through the use of the kink-fluctuation formalism in paper I. This can yield information on the friction coefficient, and throw light on the validity of the actual behavior of the forces exerted by the thermal fluctuations (e.g., are they

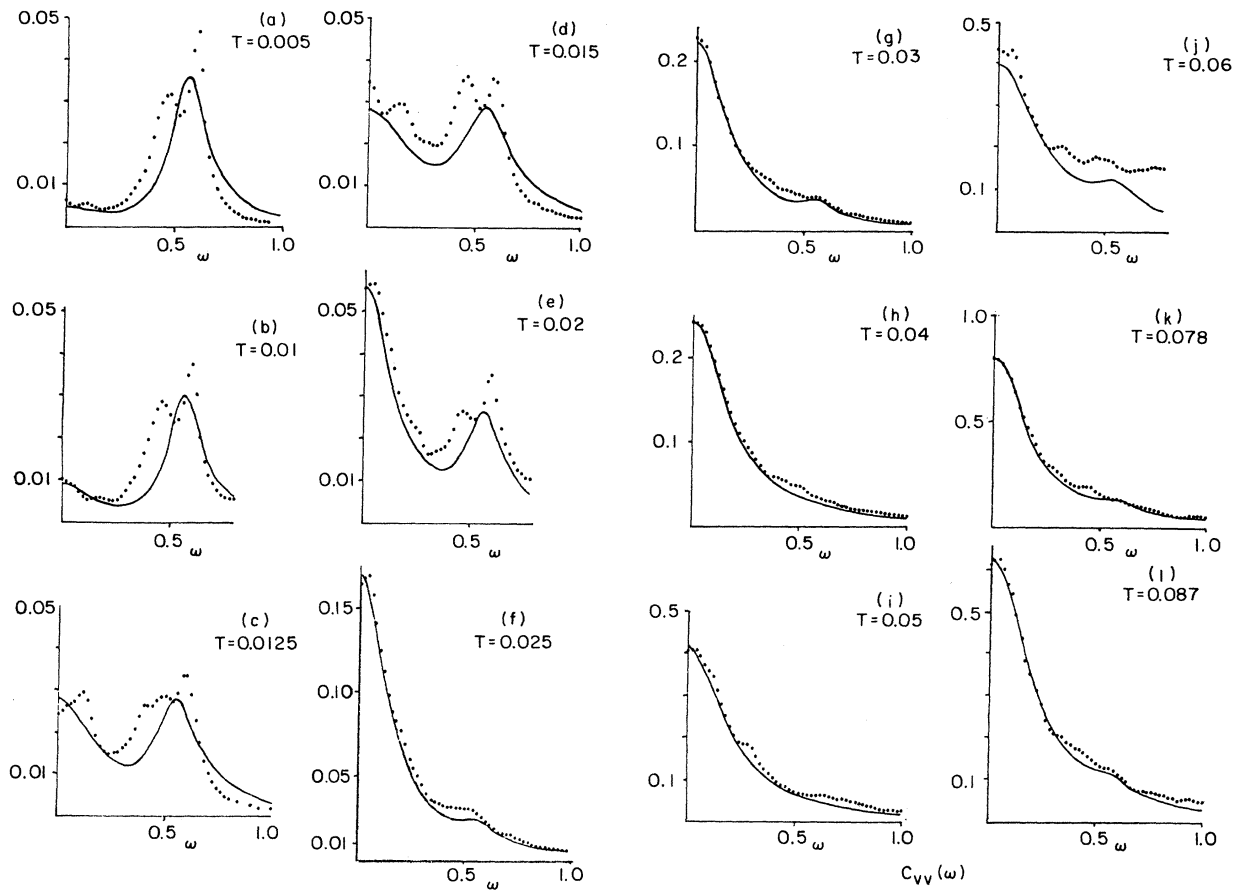


FIG. 4. Fourier transform $\hat{\psi}(\omega)$ for $\bar{C}=0.5$ at various temperatures. Solid circles represent transform of raw data; curves are the transforms of the solid curves in Fig. 3.

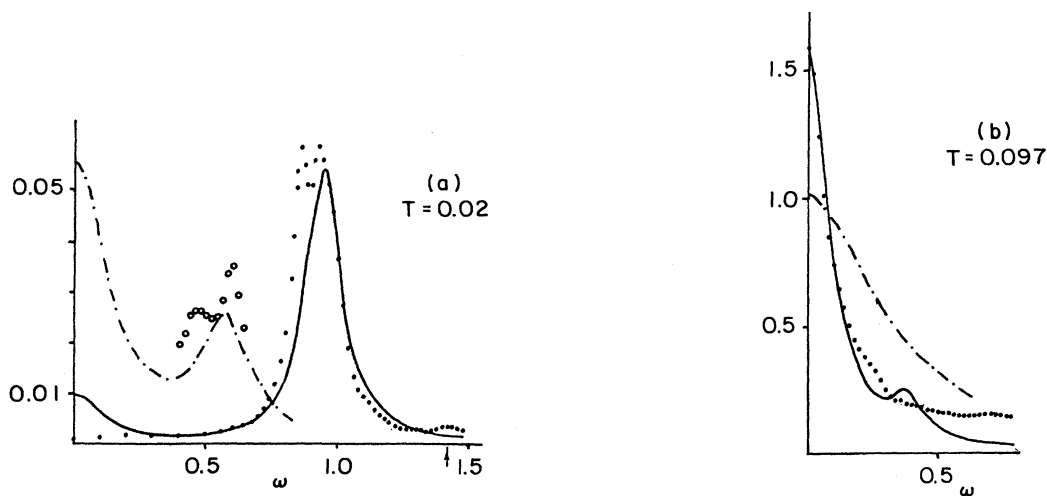


FIG. 5. Same as Fig. 4 comparing $\hat{\psi}(\omega)$ for different \bar{C} values. (a) $\bar{C}=0.5$ (open circles and dashed-dot line) and $\bar{C}=0.2$ (points and solid curve) at $T=0.02$. Arrow denotes position of continuum peak predicted by Sahni and Mazenko (see text). Note the increase in the oscillatory peak frequency as \bar{C} is increased. The diffusion constant $\hat{\psi}(0)/2$ drops drastically as \bar{C} is lowered. (b) $\bar{C}=0.5$ (dashed-dot line) and $\bar{C}=0.7$ (points and solid curve) at $T=0.097$. Dynamics are dominated by diffusion; the oscillatory peak disappears. The diffusion increases with \bar{C} .

Markovian, and is there memory in the dissipation?). The thermal lattice can be generalized to incorporate external forces.⁶ This can also yield information about the coupling of kinks to constant and time-dependent external fields. Since kink motion is dissipative, its coupling to external fields can yield information on internal friction and plasticity in solids. Multiple kink phenomena have been avoided here, but extension of simulation and theory to include effects of many interacting kinks must be

made, since kink-kink interactions may have significant equilibrium and nonequilibrium effects.

ACKNOWLEDGMENTS

This work was supported by the Army Research Office and the National Science Foundation. One of us (S.Y.) would like to thank T. R. Koehler for suggesting the use of the antiperiodic boundary condition.

-
- ¹S. Aubry and R. Pick, *Ferroelectrics* **8**, 471 (1974); W. Hasenfratz and R. Klein, *Physica (Utrecht)* **89**, 191 (1977); W. C. Kerr, *Phys. Rev. B* **19**, 5773 (1979); T. R. Koehler, A. R. Bishop, J. A. Krumhansl, and J. R. Schrieffer, *Solid State Commun.* **17**, 1515 (1975); T. Schneider and E. Stoll, *Phys. Rev. Lett.* **35**, 296 (1975).
- ²J. A. Krumhansl and J. R. Schrieffer, *Phys. Rev. B* **11**, 3535 (1975).
- ³Y. Wada and J. R. Schrieffer, *Phys. Rev. B* **18**, 3897 (1978).
- ⁴P. S. Sahni and G. F. Mazenko, *Phys. Rev. B* **20**, 4674 (1979).
- ⁵M. A. Collins, A. Blumen, J. F. Currie, and J. Ross, *Phys. Rev. B* **19**, 3630 (1979); J. F. Currie, A. Blumen, M. A. Collins, and J. Ross, *Phys. Rev. B* **19**, 3645 (1979).
- ⁶J. A. Combs, Ph. D. thesis, Department of Nuclear Engineering, M. I. T., 1981 (unpublished).
- ⁷J. A. Combs and S. Yip, *Phys. Rev. B* **28**, 6873 (1983), henceforth referred to as paper I.
- ⁸J. F. Currie, S. E. Trullinger, A. R. Bishop, and J. A. Krumhansl, *Phys. Rev. B* **15**, 5567 (1977).
- ⁹J. M. Dickey and H. Paskin, *Phys. Rev.* **188**, 1407 (1969).
- ¹⁰E. Tomboulis, *Phys. Rev. D* **12**, 1678 (1975).
- ¹¹M. C. Wang and G. E. Uhlenbeck, in *Noise and Stochastic Processes*, edited by N. Wax (Dover, New York, 1954).